JTTEE5 22:36–47
DOI: 10.1007/s11666-012-9831-5
1059-9630/$19.00 © ASM International

Improvement of Adhesion and Cohesion in Plasma-Sprayed Ceramic Coatings by Heterogeneous Modification of Nonbonded Lamellar Interface Using High Strength Adhesive Infiltration

Guan-Jun Yang, Chang-Jiu Li, Cheng-Xin Li, Katsuyoshi Kondoh, and Akira Ohmori

(Submitted April 18, 2012; in revised form September 4, 2012)

The mechanical properties and related performance of thermally sprayed ceramic coatings are degraded by their relatively low adhesion and cohesion resulting from the limited bonding at substrate/splat interface and splat/splat interface. In this study, the influence of high strength adhesive infiltration on the microstructure and erosion performance of plasma-sprayed Al_2O_3 coatings was investigated to understand the improving mechanism of adhesion and cohesion through heterogeneous modification of nonbonded interfaces. Element distribution maps proved that the adhesive can be infiltrated from the coating surface to the coating/substrate interface through the inter-connected open pores including in-plane nonbonded area and microcracks in splats. Both adhesion and cohesion can be significantly improved by the heterogeneous modification of nonbonded lamellar interfaces of both splat/splat and splat/substrate through adhesive infiltration. The adhesive strength of the coating was increased from several MPa to ~50 MPa after adhesive infiltration. The erosion resistance at a large particle jet angle was improved by a factor of 3 due to the significant improvement of the lamellar cohesion, although the erosion resistance at a small particle jet angle was not significantly influenced.

Keywords adhesive infiltration, adhesive strength, ceramic coating, cohesion, erosion resistance, plasma spraying

1. Introduction

The adhesion and cohesion are most important issues with regard to the applications of thermally sprayed coatings (Ref 1). For a thermally sprayed coating used under a certain mechanical loading, the coating delamination or spallation off in service may be caused by the weak adhesion at coating/substrate interface and the limited lamellar cohesion at splat/splat interface in the coating. This certainly leads to the decrease in coating effective thickness or even the direct exposure of the substrate surface to operating environment.

The adhesion of plasma-sprayed ceramic coating is usually limited to mechanical interlocking effect between coating and substrate. Berndt and Ostojic reported the mean adhesive strength of 2.3, 4.7, and 7.8 MPa for Al_2O_3-2.5%TiO_2, ZrO_2-5%CaO, and ZrO_2-6%Y_2O_3 coatings, respectively (Ref 2). Hasui et al. reported that the adhesive strength of Al_2O_3 coatings was increased from 6 to 11 MPa with the increase of substrate preheating to 380 °C (Ref 3). In addition, the adhesive strength can also be improved by using a Ni-Al bond coat between the ceramic coating and substrate (Ref 4, 5). It has been clearly found that the voids in the coating influence many properties such as mechanical, physical (e.g., thermal conductivity), and chemical (e.g., corrosion) properties of the deposits (Ref 6-8). By sealing the voids using sealant infiltration, the open pores in the coating can be well sealed up by sealant, and consequently the corrosion resistance of the coatings is significantly improved (Ref 9, 10). Many experiments revealed that the failure of the coating occurs easily from the interfaces between lamellae in the coating, for example under a localized load such as in abrasive wear (Ref 11, 12), erosion (Ref 13), and fracture mechanics test (Ref 14-16). Such effect is attributed to the pores in the coating in the form of nonbonded lamellar interface (Ref 6), although the existence of the nonbonded lamellar interface leads to a low thermal conductivity and a high thermal barrier performance for plasma-sprayed ceramic thermal barrier coatings (Ref 6). Therefore, the modification of the lamellar microstructure of the as-sprayed coating is desirable to improve the coating performance.

Guan-Jun Yang Chang-Jiu Li and **Cheng-Xin Li**, State Key Laboratory for Mechanical Behavior of Materials, School of Materials Science and Engineering, Xi'an Jiaotong University, Xi'an, Shaanxi 710049, China; and **Katsuyoshi Kondoh** and **Akira Ohmori**, Welding and Joining Research Institute, Osaka University, Ibaraki, Osaka Japan. Contact e-mail: licj@mail.xjtu.edu.cn.

The limited bonding condition between the splats has been regarded as one of the most essential structural characteristics of thermally sprayed ceramic coatings. The maximum bonding ratio between the lamellae is only ~32% for plasma-sprayed ceramic coatings without special substrate heating (Ref 6, 17-19), although a variety of spraying conditions, including spray method, plasma arc power, etc., have been significantly changed to aim at improving splat bonding. Through controlling splat or substrate surface temperature prior to droplet impact, the splat bonding ratio in YSZ coating can be significantly increased by keeping the deposit surface at a high temperature of >800 °C, and thereby both mechanical properties and physical properties such as electric conductivity can be significantly improved (Ref 20-22). Nevertheless, the improvement of nonbonded interface in conventional thermally sprayed ceramic coatings is of significant importance to aim at further enhancing the coating property and performance.

Up to now, many attempts have been made to modify the coating microstructure, and most of them focus on the decrease of the overall coating porosity through a high temperature processing, including laser remelting treatment (Ref 23-33), various heat treatment (Ref 34-41), ceramic infiltrating treatment (Ref 42-55), organic sealant infiltration (Ref 56-63), and liquid metal infiltration (Ref 64-66). All these modification processes have certain advantages to improve coating performance. However, a high temperature up to the melting point of the coating material is often required for those coating modification processes, which significantly limits the industrial applications of those approaches. Our previous results showed that the erosion resistance of the plasma-sprayed Al_2O_3 coating can be improved by adhesive infiltration (Ref 63). As for the understanding of the sealing process and sealing mechanism, the most accepted idea is mainly based on the sealing of the open pores (Ref 9, 59, 61). Actually, this theory well explains the significant improvement of the corrosion resistance of the plasma-sprayed ceramic coatings. The mechanical property and related performance need further in-depth examination, although some references deduced the modification of lamellar microstructure without providing direct experiment evidence (Ref 50, 57, 58, 60, 63).

In the present paper, the influence of high strength adhesive infiltration on the adhesion and cohesion of plasma-sprayed alumina coating was examined. The cohesion improvement was correlated with the erosion performance of the adhesive-infiltrated coatings to aim at understanding the dominant mechanism of the heterogeneous modification of lamellar structure. The low temperature, <200 °C, of this approach will lead to energy saving and promising industrialization of the enhancement of the mechanical property and related performance.

2. Experimental Procedures

2.1 Coating Deposition

Spray feedstock was commercially available Al_2O_3 powders (K-16T, ShowaDenko, Japan) of a particle size from 10 to 44 μm. Both stainless steel and mild steel were used as substrates to reveal the effect of substrate type on adhesive strength of coatings. The substrates were sand-blasted by alumina grits prior to spraying.

Al_2O_3 coating was deposited by SG-100 torch (Plasmadyne, USA) at a plasma arc power of 30 kW. Argon at a pressure of 0.42 MPa was used as primary gas, and helium at a pressure of 0.63 MPa was used as secondary gas. The spray distance was fixed at 150 mm. Two types of test pieces were prepared. One type of specimen was used for tensile adhesion test that had dimensions of 25.4 mm in diameter and 25.4 mm in length following ASTM C-633 standard. The other type of specimen was those deposited on steel plates that had the dimensions of 50 × 60 × 6 mm for the particle erosion test and microstructural examination of the coating.

For some test pieces, Ni-20Cr bond coat of 80 μm thickness was deposited between the substrate and Al_2O_3 coating to reveal the effect of bond coat on adhesive strength of coatings. For Ni-20Cr bond coat, plasma spraying was carried out with Metco 9MB torch under plasma power of 33 kW and spray distance of 150 mm. The temperature of the substrate surface prior to deposition and the coating surface during deposition was monitored by an infrared thermometer.

2.2 Adhesive Infiltration and Coating Characterization

To investigate the influence of adhesive type on the infiltration and performance of the infiltrated coatings, type-A adhesive (Plasmatex Klebbi, Plasma-Technik, Switzerland) and type-B (E-7, Shanghai Research Institute of Synthetic Resins, China) adhesive, shown in Table 1, were used as infiltrates for comparison. The liquid type infiltrates were brushed on the coating surface and then cured in ambient atmosphere under the conditions of 180 °C × 2 h and 200 °C × 2 h for type-A and type-B, respectively. The low viscosity of the adhesives at these relatively high temperatures would allow the infiltration of liquid adhesives into the pores of the coatings. The two epoxy adhesives used in this study show a relative high tensile strength of ~60 MPa, and could be used at a maximum temperature of 200 °C with no claim of significant corrosion resistance.

The adhesive strength of both the as-sprayed and the adhesive-infiltrated Al_2O_3 coatings was measured by tensile test following ASTM C-633 standard at a cross-head speed of 1 mm/min. Solid sheet adhesive (FM1000, Cytec, USA, referred as type-C) was used as the glue to bond the coating specimen and the couple specimen. The curing condition shown in Table 1 was selected according to the suggestion of the manufacturer. Each mean strength was obtained by using at least three specimens.

The erosion resistance of the coatings was examined by particle erosion test using a commercial ACT-JP erosion tester (Arata coating tester with jet particles, Takahashi Engineering, Kobe, Japan) (Ref 67). A certain amount of alumina abrasive for each test was accelerated by the compressed air at a flow rate of 340 L/min and a pressure

Table 1 The adhesives used in the study

Type	Commercial code	Chemical	State*	Curing condition	Purpose
A	Plasmatex Klebbi	Epoxy	Liquid	180 °C × 2 h	Infiltrate
B	E-7	Amino-epoxy with four functional groups	Liquid	200 °C × 2 h	Infiltrate
C	FM 1000	Polyamide-epoxy	Solid sheet	170 °C × 1 h	Glue

* The state refers to the state of adhesive at room temperature condition

of 0.5 MPa through a nozzle of 3.6 mm in diameter. After each test, the weight loss of the coating was measured. The overmuch adhesive on the adhesive-infiltrated coating surface was eliminated using a sand paper prior to the erosion test.

The microstructure of the coatings was characterized by scanning electron microscopy (SU-70, Hitachi, Tokyo, Japan, and QUANTA 600F, FEI, USA). To reveal the adhesive infiltration, the element distribution map was measured by an energy dispersive spectrometer (EDS) (INCA Wave, Oxford, Oxon, UK) equipped on the scanning electron microscope.

3. Results

3.1 Adhesive Strength of Plasma-Sprayed Al_2O_3 Coatings

Table 2 shows the adhesive strength of the Al_2O_3 coatings deposited under different conditions on mild steel substrate measured using solid sheet adhesive (type-C). The as-sprayed coating without substrate preheating and bond coat yielded an adhesive strength of 6.5 MPa. Similar results were also reported by other investigators (Ref 2-4). A little increase in adhesive strength was observed when the NiCr bond coat was applied. Moreover, the preheating of the substrate prior to coating deposition also contributed to the increase of the adhesive strength. These results are consistent with those reported by other investigators (Ref 3, 4). It can be found that plasma-sprayed Al_2O_3 coatings exhibited a limited mean adhesive strength from 6.5 to 12.8 MPa.

3.2 Effect of Adhesive Infiltration on the Microstructure of Al_2O_3 Coatings

Figure 1 shows the typical cross-sectional microstructure of both the as-sprayed Al_2O_3 coating and the infiltrated Al_2O_3 coatings. Compared to the as-sprayed coating, the infiltrated coatings presented a denser microstructure (Note: the polishing condition for all types of coatings was the same). Since the apparent large pores on the cross-section of the as-sprayed coating resulted from the spalling off of splats during the polishing process of the sample (Ref 68, 69), the dense microstructure implies that the adhesive has infiltrated into the whole thickness of the coating and protected the splats from spalling off during sample preparation. This result is consistent well with the proposed microstructure examination approach with the resin infiltration prior to sample sectioning (Ref 69).

Table 2 Adhesive strength of the Al_2O_3 coatings on mild steel substrate

Preheating Temp., °C	Thickness, μm	Mean tensile strength, MPa
Non	500	6.5 ± 1.1
Non	80* + 500	11.3 ± 2.3
250	500	12.8 ± 2.9

* The thickness of Ni-20Cr bond coat

3.3 Effect of Adhesive Infiltration on the Adhesive Strength of Al_2O_3 Coatings

Table 3 shows the adhesive strength of the type-A adhesive-infiltrated Al_2O_3 coatings deposited on both stainless and mild steel substrates under different preheating temperatures. It can be found that the mean adhesive strength achieved 40 to 51 MPa for the infiltrated coatings. Moreover, it can be recognized that the apparent adhesive strength of the adhesive-infiltrated coatings was little influenced by the deposition conditions including substrate type, substrate preheating, and bond coat application, etc. The examination of the fractured surface showed that the fracture of most coatings occurred at the Al_2O_3/substrate interface (Al_2O_3/bond coat interface for the coatings with bond coat) with a limited fraction of fracture within the coating. With the coating deposited without substrate preheating and bond coat, the adhesive strength of the infiltrated coating was significantly increased by a factor of 5-10.

3.4 Effect of Adhesive Infiltration on the Erosion Resistance of Al_2O_3 Coatings

Figures 2 and 3 show the relationships between the total weight loss of the coating and the abrasive weight for the as-sprayed coating and the adhesive-infiltrated coatings at a jet angle of 90° and 30°, respectively. The test was continued until the substrate surface was clearly observed for the as-sprayed coating and the type-A adhesive-infiltrated coating, while the test was stopped for the type-B adhesive-infiltrated coating when the tests were carried out long enough to obtain the representative erosion rate. For the erosion tests at both jet angles, the total weight loss of the type-A adhesive-infiltrated coating was comparable to that of the as-sprayed coating. The visual

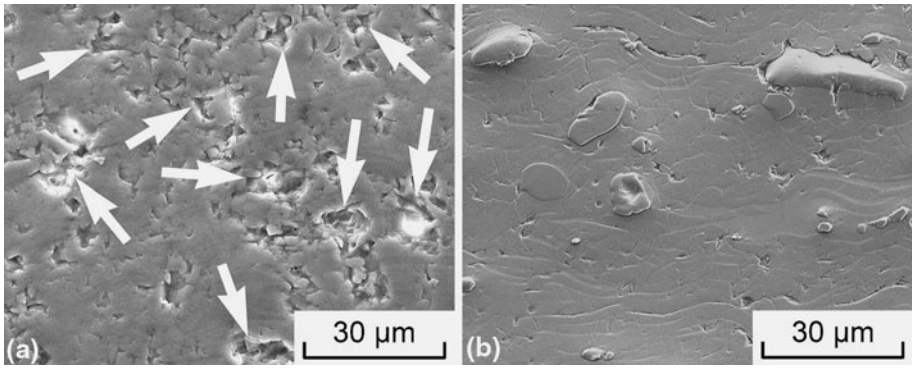

Fig. 1 Microstructure of both as-sprayed Al_2O_3 coating and type-A adhesive-infiltrated Al_2O_3 coating. (a) as-sprayed coating, (b) infiltrated coating

Table 3 Adhesion test results of the Al_2O_3 coatings infiltrated with type-A adhesive

Substrate	Preheating temp., °C	Thickness, μm	Tensile strength, MPa
Stainless steel	Non	80* + 500	39.5 ± 7.8
Stainless steel	Non	500	47.4 ± 10.5
Stainless steel	260	500	40.4 ± 6.8
Stainless steel	350	500	43.6 ± 3.9
Mild steel	310	500	50.6 ± 2.7

* The thickness of Ni-20Cr bond coat

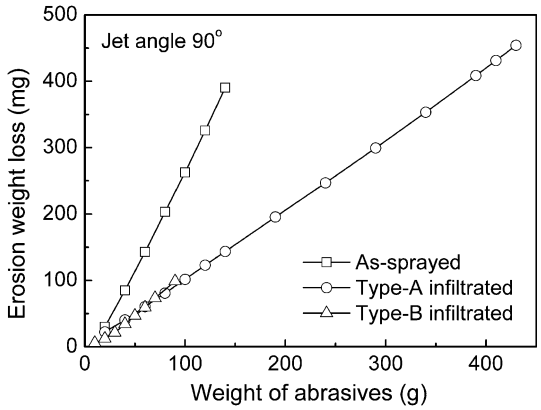

Fig. 2 Relationships between the abrasive weight and the total weight loss for the as-sprayed Al_2O_3 coating and two infiltrated Al_2O_3 coatings at a jet angle of 90° (The data of the as-sprayed coating and type-A adhesive-infiltrated coating were after Ref 63)

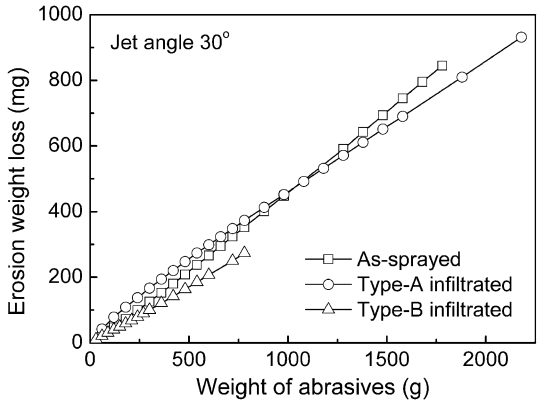

Fig. 3 Relationships between the abrasive weight and the total weight loss for the as-sprayed Al_2O_3 coating and two infiltrated Al_2O_3 coatings at a jet angle of 30°

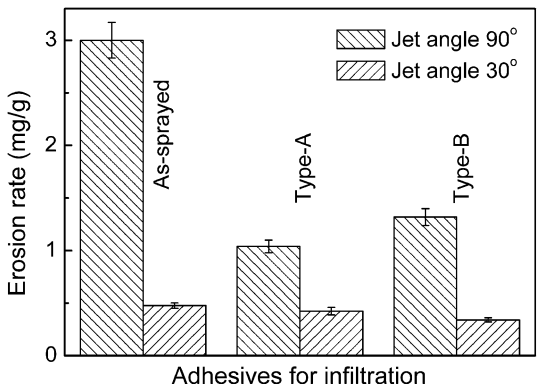

Fig. 4 Comparison of the erosion rate of as-sprayed Al_2O_3 coating with those of the adhesive-infiltrated coatings

morphology of the eroded coating surface presented a typical ball impression morphology (ball impression for a jet angle of 90°, and ellipsoid impression for a jet angle of 30°) corresponding to the distribution of the abrasive particles in the particle jet. In the case of jet angle of 90°, 150 g abrasives were required to erode off the as-sprayed coating, while 450 g abrasives were required for the type-A adhesive-infiltrated coating. However, in the case of jet angle of 30°, the abrasives acquired to erode off the coatings were comparable for the as-sprayed and infiltrated coatings.

The erosion rate was defined as the coating weight loss divided by the abrasive weight at a steady state of erosion wear test shown in Fig. 2 and 3. At least five tests were used to obtain the erosion rate in this study. Figure 4

shows the comparison of the erosion rates of the as-sprayed and adhesive-infiltrated coatings. Compared to the as-sprayed coating, the erosion rates at a jet angle of 90° for the two adhesive-infiltrated coatings were much lower by about one-third. In addition, the adhesive type showed only a little effect on the erosion rate of the adhesive-infiltrated coatings, since both adhesives have comparable strength. Therefore, it is clear that the erosion resistance of plasma-sprayed coating after infiltration is significantly improved by a factor of ~3 for both adhesives. However, in the case of 30° jet angle, the erosion rates for the as-sprayed coating and the adhesive-infiltrated coatings were comparable.

4. Discussion

4.1 The Open Pore Structure of Plasma-Sprayed Ceramic Coating and Sealing Treatment

A thermally sprayed deposit is generally of lamellar structure shown in Fig. 5 (Ref 17). A fraction of pores from several percent to ~20% can be formed in the deposit (Ref 70). The plasma-sprayed ceramic coatings consist of three types of pores. One type is large pores in micrometer size, which results from insufficient filling of the droplets to the previously formed rough deposit surface. The second type is the interlamellar pores resulting from incomplete wetting of molten liquid to the previously deposited splat surface. It was reported that the bonding ratio between the lamellae is only as low as ~32% for plasma-sprayed ceramic coatings (Ref 6, 17-19). This means that most of the interface between lamellae is in the form of nonbonded area, e.g., interlamellar pores which are depicted by the white strings between ceramic splats shown in Fig. 5. The low bonding ratio results in the low adhesion and cohesion for the plasma-sprayed coatings. Additionally, the microcracks perpendicular to splat surface can be formed easily in the splats owing to quenching stress (Ref 71). Such cracks often penetrate through the whole splat and contribute to the interconnecting of pores in the coating.

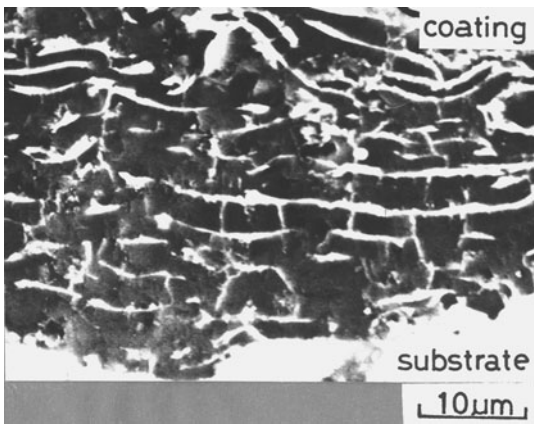

Fig. 5 Pore structure of the plasma-sprayed Al_2O_3 coating visualized by the electroplated Cu (after Ref 17)

The crossing and connection of these three types of pores contribute to an inter-connected pore structure from the coating surface to the coating/substrate interface. This is the reason for the poor corrosive resistance of the plasma-sprayed ceramic coatings on metallic substrate (Ref 9, 10, 46, 59, 61, 72), although ceramic material has excellent intrinsic corrosion resistance. Although the open porosity is proposed to decrease with the increase of coating thickness based on the decrease of the corrosion current with increasing coating thickness (Ref 72), the gas permittivity, which depends only on connected open pores, of plasma-sprayed coatings is independent of coating thickness (Ref 43-45, 73, 74). Quantitative investigation showed that more than 90% of the total pores in plasma-sprayed ceramic coatings are in the form of open pores which are well connected to each other (Ref 75).

The connectivity of the pores in the coating provides an opportunity to allow the infiltration of some substances into the pores. As a typical and successful example, copper is electroplated into the pores in plasma-sprayed Al_2O_3 coatings, leading to a quite clear visualization of the pore structure and thereby a systematic qualitative and quantitative evaluation of coating microstructure (Ref 6, 17-19, 76). A large number of references proved that the corrosion resistance of the coating is significantly enhanced by the sealing of pores via the infiltration of various organic and inorganic sealants (Ref 42-63). Because the corrosion resistance of the coating depends on the overall connectivity of the open pores, it is effective to just make the open pores to be the close pores even in a limited depth of the coating surface, rather than the whole thickness (Ref 9, 10). Actually, TEM results show that the open pores are not fully eliminated, and there are still a large amount of closed pores left in the coating (Ref 45, 46, 50). It can be clearly found that at least some, or even most, of the nonbonded lamellar interfaces between splats are kept at unconnected state (Ref 45, 46, 50).

4.2 The Strengthening of Lamellar Cohesion and Coating/Substrate Adhesion

The adhesive strength of plasma-sprayed ceramic coatings is usually measured by tensile test according to the standards such as ASTM C633-79, DIN 50-160-A, AFNOR NF A91-202-79, and JIS H8666-80. The test results may be different by a factor of 10 among different investigations (Ref 2, 3). It can be found that the adhesive strength of the as-sprayed Al_2O_3 coatings measured in the present study is well consistent with those reported results (Ref 2, 3). To increase the adhesive strength, several approaches have been proposed. The utilization of thermally sprayed metallic bond coat can increase the adhesive strength a little according to this study and other literature (Ref 4, 5). As the reason of this increment, besides the higher surface roughness of the bond coat than bare substrate (Ref 4), the surface oxide formed on the thermally sprayed bond coat would also be an important factor that allows better wettability between the bond coat surface and ceramic droplet (Ref 77). In addition, the increase in the substrate temperature also leads to an

increase of adhesive strength, shown in Table 2. This could be attributed to the elimination of the splat splashing by the desorption of the adsorbates on substrate surface (Ref 78-80) and the formation of thicker oxide layer on the substrate surface (Ref 76). Taking these two approaches into account, the adhesive strength of thermally sprayed ceramic coatings is still in the magnitude of ~10 MPa.

This relatively low adhesion could be attributed to that the crack often propagates along the nonbonded area at splat/splat interface or more often at the coating/substrate interface which is a typical heterogeneous interface with different material types. Note that the coating/substrate interface herein refers to the Al_2O_3/substrate interface or Al_2O_3/bond coat interface. Therefore, the improvement of the adhesive strength needs the adhesive infiltration throughout the coating to reach to the coating/substrate interface.

To prove the infiltration of the adhesive into the coating, element distribution maps were measured by EDS mapping as shown in Fig. 6. Figure 6(a) and (b) shows that a pore with a size of several micrometers is present within the coating near the coating surface. It can be clearly observed from Fig. 6(c) that carbon was present in the pore, which indicates that the adhesive has been infiltrated into the pore from the outside of the coating surface. Figure 6(d) shows the element distribution map for the microcracks (marked with larger arrows) in splats and nonbonded area (marked with smaller arrow) between lamellae. It can be found that both the cracks and nonbonded area were filled in by adhesive. These results clearly demonstrate that the adhesive has been successfully infiltrated into the pores within the coating through the microcracks in splats and nonbonded area between lamellae, which were inter-connected to each other.

Figure 7 shows the element distribution maps in the coating/substrate interface region. The map shown in Fig. 7(c) reveals that the pore in the coating/substrate interface is filled with the adhesive that is infiltrated from the outside of the coating through the nonbonded area between lamellae and vertical cracks in splats. It can also be clearly found from Fig. 7(d) that the pore with a size of several micrometers is full of adhesive. Therefore, the results clearly proved the complete infiltration of adhesive into the coating/substrate interface.

With the infiltration of adhesive into the nonbonded area in a size of sub-micrometer at the interfaces between the coating and substrate, the adhesive forms a strong bonding between the coating and substrate surface. Accordingly, the apparent adhesive strength of the adhesive-infiltrated coating is significantly increased to 40-51 MPa from several MPa of the as-sprayed coatings. Kim et al. also reported that the adhesive strength of plasma-sprayed Al_2O_3-TiO_2 coating increased from ~5 to 35~40 MPa after organic sealants infiltration (Ref 58). Furthermore, the test results are little influenced by deposition conditions, including substrate type, substrate preheating temperature and bond coat, and mainly dependent on the strength of the adhesive, i.e., ~60 MPa for type-A adhesive. This strength is about 5 to 10 times higher compared to that of the as-sprayed coating.

However, the adhesive strength of the as-sprayed ceramic coatings from 30 to 60 MPa can also be found in some reports (Ref 81-86). It can also be recognized that these results of nearly one order higher than those mentioned above for the as-sprayed coatings are coincident with those of the adhesive-infiltrated ceramic coatings shown in Table 3. This coincidental agreement implies the uncertainty with the true adhesive strength of thermally sprayed ceramic coatings when the test is performed using liquid type adhesives which easily penetrate through the coating and reach the coating/substrate interface.

To further prove the strengthening of the cohesion between the splats by the adhesive, the fractured cross-section of the coatings was observed and shown in Fig. 8. A typical lamellar structure presenting some nonbonded regions (marked by white arrows) can be clearly recognized from the as-sprayed coating shown in Fig. 8(a), since the nonbonded regions contribute to the uneven fracture of the splats. However, the fracture surface of the adhesive-infiltrated coating shown in Fig. 8(b) presented a relatively smoother topographical morphology. Seldom nonbonded regions between splats could be recognized. This indicates the healing of the nonbonded interface by the adhesive infiltrated. In brief, the adhesive infiltrated into the pores fills in the nonbonded splat/splat interface and nonbonded Al_2O_3/substrate interface, resulting in the strengthening of the cohesion and adhesion of the coating.

4.3 Effect of Lamellar Cohesion Strengthening on Erosion Performance

The lamellar bonding in plasma-sprayed alumina coating could only be attained to one-third without a special substrate preheating (or deposit surface heating), for example, to >800 °C for YSZ coating (Ref 17, 87). Such limited cohesion leads to the erosion of coating through lamellar debonding at a high jet angle, since the splats would spall off under the repeated impacts of abrasive particles (Ref 13, 25, 88-90). Quantitative investigation showed that the erosion resistance (the reciprocal of erosion rate) was linearly proportional to the bonding ratio between splats (Ref 87, 91). It can be clearly found from Fig. 4 that the erosion rates at a jet angle of 90° were significantly reduced by the adhesive infiltration for both type-A adhesive and type-B adhesive. Accordingly, the present results clearly reveal that the strengthening of the lamellar cohesion by adhesive infiltration contributes to the significant improvement of the erosion resistance of the coating under a condition of high jet angle.

Janos et al. reported that the erosion rate of plasma-sprayed 7YSZ coatings decreases to 1/3-1/5 through heat treatment for 16 h at 1482 °C (Ref 37). The contact area between the splats in the coating increases after the heat treatment (Ref 37-41), and nearly an isotropic homogenous microstructure is observed compared with the typical lamellar structure of the as-sprayed coating (Ref 37). Therefore, the improvement of erosion resistance with a normal jet angle by a factor of 3 in this study may imply that, from the point view of contributing to the cracking resistance during erosion wear service, the interface areas

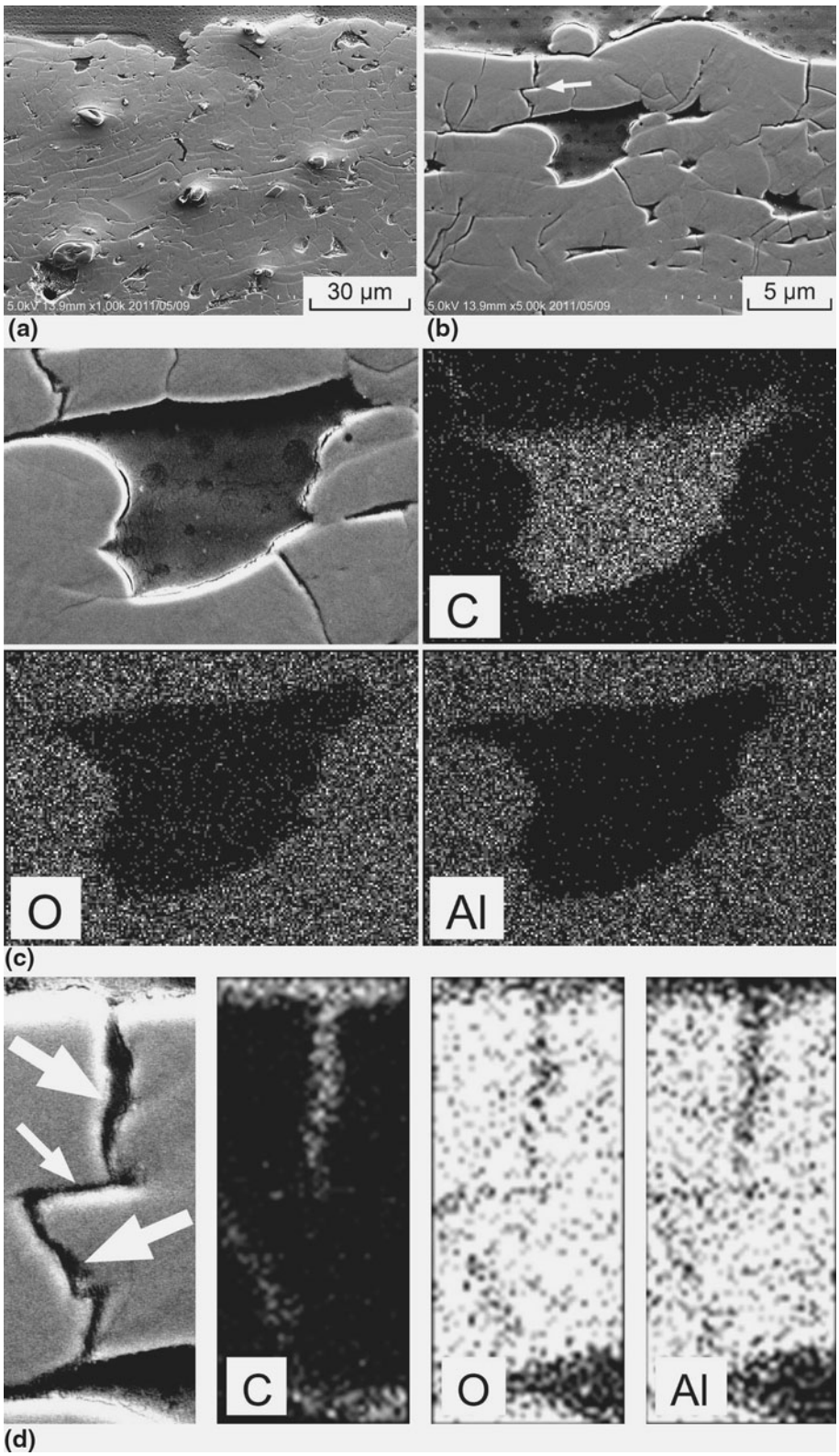

Fig. 6 Element distribution of the large pore and cracks within the coating. (a) Cross-section at low magnification, (b) cross-section at high magnification, (c) element distribution in the large pore, and (d) element distribution in the nonbonded area between splats and vertical cracks in splats

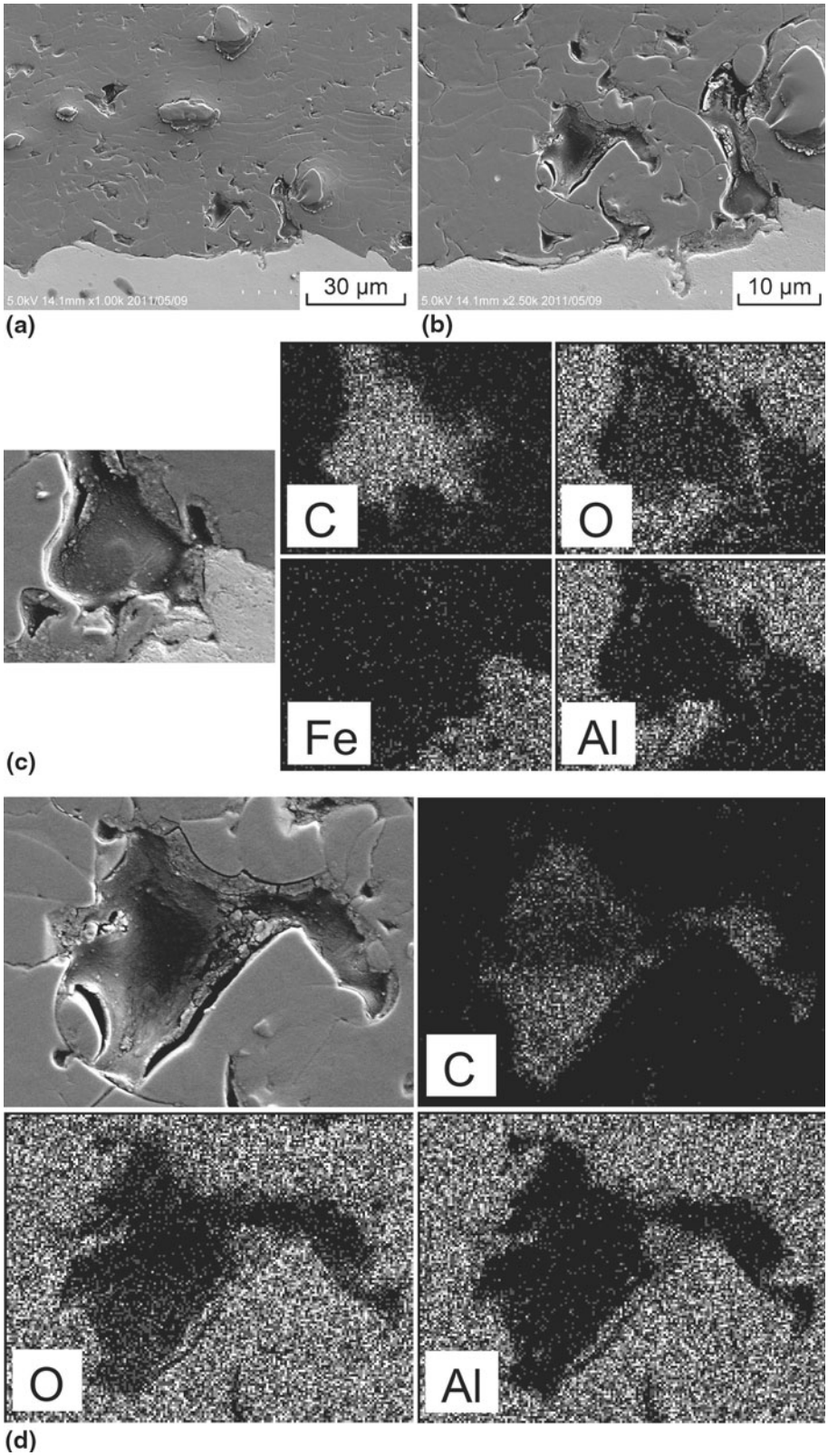

Fig. 7 Element distribution of the large pore and coating/substrate interface within the coating. (a) Cross-section at low magnification, (b) cross-section at high magnification, (c) element distribution in the pore at coating/substrate interface, and (d) element distribution in the large pore

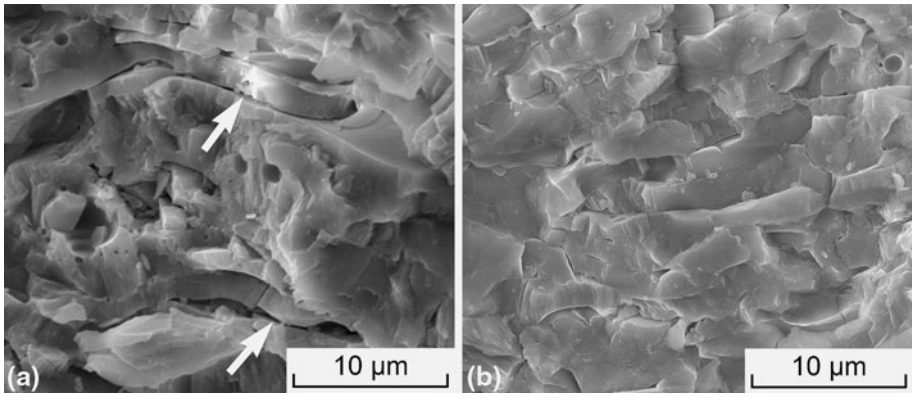

Fig. 8 Fractured cross-section of both as-sprayed Al_2O_3 coating and type-A adhesive-infiltrated Al_2O_3 coating. (a) As-sprayed coating, (b) infiltrated coating

bonded by infiltrated adhesive present a comparable cohesion to the bonded Al_2O_3 lamellar interface, which is formed during the plasma spraying process. It can also be recognized that the improvement of the erosion performance of the coating depends on the adhesive type (type-A adhesive seems more effective than type-B adhesive). Further detailed work may be carried out for the optimization of adhesive type and curing condition.

The linear relation between the erosion weight loss of the coating and the weight of abrasives clearly indicates that the eroded part of the coating is of a homogeneous cohesion between the lamellae. For the type-A adhesive-infiltrated coating, the linear relation observed for the whole erosion test lasting to the exposure of the coating/substrate interface suggests that the adhesive homogeneously penetrates the whole thickness of the coating.

It is worth to note that the erosion rate at a low jet angle of 30° only slightly decreases after adhesive infiltration, according to Fig. 3 and 4. This could be attributed to the different erosion mechanisms for high and low jet angles. Compared to the splat spalling off mechanism at high jet angles (Ref 13, 25, 87-89), the erosion at low jet angles is dominated by the microcutting or ploughing of splats (Ref 89). Similar to the abrasive wear, the erosion wear at low jet angles mainly depends on the hardness of the coating material. Therefore, for those infiltrations in which hard ceramic materials, such as Cr_2O_3, mullite, Al_2O_3, and aluminum phosphate, are formed in the pores of the coatings, the abrasive wear resistance could be effectively improved (Ref 47-49). However, it is also found that the abrasive wear resistance could not be significantly modified if relatively soft materials, such as organic sealants with corrosion resistance, are infiltrated in the pores of the coating (Ref 58, 60, 62).

4.4 Improving Mechanism Of Adhesion/Cohesion Through Heterogeneous Modification of Lamellar Bonding

According to the interface characteristics of non-bonded lamellae, the approaches for the modification of lamellar bonding can be divided into two groups, i.e., homogeneous and heterogeneous modification. Homogeneous modification means that the nonbonded interface between splats heals up in situ by the same material of the coating. Laser treatment (23-33), heat treatment (including hot isostatic pressing treatment (Ref 34, 35), microwave sintering (Ref 36), spark plasma sintering (Ref 38) and conventional heat treatment (Ref 37, 39-41)) are typical homogeneous modification, in which the nonbonded interface is healed up by only splats themselves. With laser treatment, the lamellar splats are melted into an integrated liquid phase, which then solidifies to a typical columnar structure due to the directional heat transfer (Ref 23-28). The nonbonded lamellar interface is completely eliminated after laser remelting treatment. On the other hand, during other types of heat treatment, the nonbonded interface is healed up by the diffusion of splat material near the crack tip at a solid state (Ref 34-41).

During the heterogeneous modification, additional materials are introduced into the nonbonded interface areas to connect the nonbonded lamellae together. The ceramic material synthesized by chemical decomposition of the precursor infiltrated in the pores can be used to modify the nonbonded interface (Ref 42-45). The ionic conductivity of plasma-sprayed YSZ coating is improved by the nano-sized YSZ particles resulting from the decomposition of zirconium nitrate infiltrated in the nonbonded interface area (Ref 44, 45). Although the gas tightness of the coating is significantly increased by more than one order (Ref 43, 44), the ionic conductivity is only enhanced by ~20% (Ref 44, 45). Microstructural examination shows that only a little fraction of nonbonded interface is connected by the synthesized nano-YSZ particles (Ref 45). This can possibly be attributed to the large volume reduction during the decomposition of the YSZ precursor. The significant remainder of the nonbonded interface could also be found in other infiltration methods, such as aluminum phosphate sealing treatment (Ref 45, 46, 50), although the infiltration process could be further optimized. Therefore, small or no volume reduction would be highly preferred during the heterogeneous modification of the nonbonded interface.

Organic sealant infiltration presents a low shrinkage, for example, <3% for typical epoxy. In the present study, adhesive with a high strength of 60 MPa is successfully infiltrated into the pores, especially nonbonded lamellar interface, throughout the whole depth of the coating from surface to coating/substrate interface. The nonbonded lamellar interface can be effectively filled with the liquid adhesive as shown in Fig. 6 and 7. Due to the limited volume shrinkage during the solidification of liquid adhesive, the pores are well filled with the solid adhesive, although a little fraction of voids can also be identified from Fig. 7(d). The nonbonded splat interface is well bonded by the high strength adhesive, which results in an effective and heterogeneous modification of the nonbonded splat interface. Consequently, the cohesion is significantly improved leading to the enhancement of the erosion resistance of the coatings after adhesive infiltration. Moreover, it also results in an effective and heterogeneous modification of the nonbonded interface between the Al_2O_3 splats and the substrate. Accordingly, the coating/substrate adhesion is significantly increased from several MPa of the as-sprayed condition to ~50 MPa after the adhesive infiltration. As a conclusion, both the cohesion and adhesion of the plasma-sprayed ceramic coatings can be effectively strengthened by the heterogeneous modification of the nonbonded lamellar interface through the infiltration of high strength adhesive. The environmental flexibility, such as low temperature and short processing time, of this approach would be expected for the industrial application in enhancing the mechanical performance, especially those significantly depending on the cohesion and adhesion of thermally sprayed ceramic coatings.

5. Conclusions

The influence of the adhesive infiltration on the adhesion and cohesion of plasma-sprayed Al_2O_3 coatings was investigated using high strength commercial adhesive. The adhesive strength of plasma-sprayed ceramic coatings was significantly improved by adhesive infiltration and reached 40-51 MPa regardless of the deposition conditions of the coatings. This means that both coating/substrate adhesion and cohesion of the coating was significantly improved by adhesive infiltration. Element distribution maps proved that the adhesive can effectively penetrate into the coating of 500 μm thickness and reach the coating/substrate interface through the nonbonded area between splats and microcracks in splats. The improvement of the adhesion and cohesion was attributed to the heterogeneous modification of nonbonded lamellar interface at both splat/substrate and splat/splat. The particle erosion resistance of plasma-sprayed ceramic coatings at an approaching jet angle of 90° was improved by a factor of 3, due to the improvement of the cohesion between lamellae in plasma-sprayed ceramic coating. However, the particle erosion resistance at a low approaching jet angle of 30° was not significantly influenced by adhesive infiltration. As a result, the enhancement of the mechanical performances related to the adhesion and cohesion can be achieved by high strength adhesive infiltration process.

Acknowledgments

The project is supported by the National Natural Science Fund for Distinguished Young Scholars of China (No.: 50725101) and Program for New Century Excellent Talents in University (No. NCET-08-0443). The authors thank Mr. Xiaotao Luo for preparing some samples in this study.

References

1. R.W. Smith, Plasma Spray Processing—The State of the Art and Future from a Surface to a Materials Processing Technology, *Proceedings of 2nd Plasma-Technik-Symposium*, S. Blum-Sandmeier, H. Eschnauer, P. Huber, and A. R. Nicoll, Ed., Lucerne/Switzerland, 1991, p 17-38
2. C.C. Berndt, and P. Ostojic, Strength Testing of Plasma Sprayed Coatings, *Proceedings of International Symposium on Advanced Thermal Spraying Technology and Allied Coatings*, 1988 (Osaka, Japan), Japan High Temperature Society, 1988, p 191-197
3. A. Hasui, S. Kitahara, and T. Fukushima, On Relation Between Properties of Coating and Spraying Angle in Plasma Jet Spraying, *Trans. Natl. Res. Inst. Met.*, 1970, **12**(1), p 9-20
4. S. Yilmaz, M. Ipek, G.F. Celebi, and C. Bindal, The Effect of Bond Coat on Mechanical Properties of Plasma-sprayed Al_2O_3 and Al_2O_3-13wt%TiO_2 Coatings on AISI, 316L Stainless Steel, *Vacuum*, 2005, **77**(3), p 315-321
5. C.R.C. Lima and R.D. Trevisan, Temperature Measurements and Adhesion Properties of Plasma Sprayed Thermal Barrier Coatings, *J. Therm. Spray Technol.*, 1999, **8**(2), p 323-327
6. C.-J. Li and A. Ohmori, Relationships Between the Microstructure and Properties of Thermally Sprayed Deposits, *J. Therm. Spray Technol.*, 2002, **11**(3), p 365-374
7. R.W. Rice, Microstructure Dependence of Mechanical Behavior of Ceramics, *Properties and Microstructure, Treatise on Materials Science and Technology*, R.K. MacCrone, Ed., Academic Press, New York, 1977, p 199-381
8. L. Pawlowski, *The Science and Engineering of Thermal Spray Coatings*, John Wiley & Sons Inc., New York, 1995, p 193
9. J. Knuuttila, P. Sorsa, and T. Mantyla, Sealing of Thermal Spray Coatings by Impregnation, *J. Therm. Spray Technol.*, 1999, **8**(2), p 249-257
10. M. Rosso, A. Scrivani, D. Ugues, and S. Bertini, Corrosion Resistance and Properties of Pump Pistons Coated with Hard Materials, *Int. J. Refract. Met. Hard Mater.*, 2001, **19**(1), p 45-52
11. P.P. Psyllaki, M. Jeandin, and D.I. Pantelis, Microstructure and Wear Mechanisms of Thermal-Sprayed Alumina Coatings, *Mater. Lett.*, 2001, **47**(1-2), p 77-82
12. J.H. Ouyang and S. Sasaki, Unlubricated Friction and Wear Behavior of Low-Pressure Plasma-Sprayed ZrO_2 Coating at Elevated Temperatures, *Ceram. Int.*, 2001, **27**(3), p 251-260
13. A. Ohmori, Y. Arata, and C.-J. Li, Basic Study on Properties of Plasma Sprayed Ceramic Coatings, *Trans. Jpn. Weld. Res. Inst.*, 1986, **15**, p 339-348
14. R. McPherson, and C.C. Berndt, A Fracture Mechanics Approach to the Adhesion of Flame and Plasma Sprayed Coatings, *Proceedings of 9th International Thermal Spraying Conference*, (Hague/Netherlands), 1980, p 310-316
15. G. Thurn, G.A. Schneider, H.A. Bahr, and F. Aldinger, Toughness Anisotropy and Damage Behavior of Plasma Sprayed ZrO_2 Thermal Barrier Coatings, *Surf. Coat. Technol.*, 2000, **123**(2-3), p 147-158
16. P.J. Callus and C.C. Berndt, Relationships Between the Mode II, Fracture Toughness and Microstructure of Thermal Spray Coatings, *Surf. Coat. Technol.*, 1999, **114**(2-3), p 114-128

17. A. Ohmori and C.-J. Li, Quantitative Characterization of the Structure of Plasma-Sprayed Al_2O_3 Coating by Using Copper Electroplating, *Thin Solid Films*, 1991, **201**(2), p 241-252
18. C.-J. Li and A. Ohmori, The Lamellar Structure of a Detonation Gun Sprayed Al_2O_3 Coating, *Surf. Coat. Technol.*, 1996, **82**(3), p 254-258
19. C. Takahashi, and T. Senda, On the Pore Structure of Plasma Sprayed Films, *Thermal Spraying: Current Status and Future Trends*, A. Ohmori, Ed., 1995 (Kobe, Japan), High Temperature Society of Japan, 1995, p 921-926
20. Y.-Z. Xing, C.-J. Li, Q. Zhang, C.-X. Li, and G.-J. Yang, Influence of Microstructure on the Ionic Conductivity of Plasma-Sprayed Yttria-Stabilized Zirconia Deposits, *J. Am. Ceram. Soc.*, 2008, **91**(12), p 3931-3936
21. Y.-Z. Xing, C.-J. Li, C.-X. Li, and G.-J. Yang, Influence of Through-Lamella Grain Growth on Ionic Conductivity of Plasma-Sprayed Yttria-Stabilized Zirconia as an Electrolyte in Solid Oxide Fuel Cells, *J. Power Sources*, 2008, **176**(1), p 31-38
22. S. Hao, C.-J. Li, and G.-J. Yang, Influence of Deposition Temperature on the Microstructures and Properties of Plasma-Sprayed Al_2O_3 Coatings, *J. Therm. Spray Technol.*, 2011, **20**(1-2), p 160-169
23. K.A. Khor, A. Vreeling, Z.L. Dong, and P. Cheang, Laser Treatment of Plasma Sprayed HA Coatings, *Mater. Sci. Eng., A*, 1999, **266**(1-2), p 1-7
24. S.O. Chwa and A. Ohmori, Thermal Diffusivity and Erosion Resistance of ZrO_2-8wt-%Y_2O_3 Coatings Prepared by a Laser Hybrid Spraying Technique, *Thin Solid Films*, 2002, **415**(1-2), p 160-166
25. P.C. Tsai, J.H. Lee, and C.L. Chang, Improving the Erosion Resistance of Plasma-sprayed Zirconia Thermal Barrier Coatings by Laser Glazing, *Surf. Coat. Technol.*, 2007, **202**(4-7), p 719-724
26. H.C. Cheng, Z.X. Li, and Y.W. Shi, Effects of TIG Surface Treating on Microstructural Characteristics and Mechanical Properties of Al_2O_3-TiB_2 Coating by APS, *Mater. Sci. Technol.*, 2011, **27**(1), p 194-200
27. A.P. Ilyuschenko, V.A. Okovity, N.K. Tolochko, and S. Steinhauser, Laser Processing of ZrO_2 Coatings, *Mater. Manuf. Processes*, 2002, **17**(2), p 157-167
28. G. Antou, G. Montavon, F. Hlawka, A. Cornet, C. Coddet, and F. Machi, Modification of Thermal Barrier Coating Architecture by In Situ Laser Remelting, *J. Eur. Ceram. Soc.*, 2006, **26**(16), p 3583-3597
29. R. Krishnan, S. Dash, R. Kesavamoorthy, C.B. Rao, A.K. Tyagi, and B. Raj, Laser Surface Modification and Characterization of Air Plasma Sprayed Alumina Coatings, *Surf. Coat. Technol.*, 2006, **200**(8), p 2791-2799
30. C. Batista, A. Portinha, R.M. Ribeiro, V. Teixeira, M.F. Costa, and C.R. Oliveira, Morphological and Microstructural Characterization of Laser-Glazed Plasma-Sprayed Thermal Barrier Coatings, *Surf. Coat. Technol.*, 2006, **200**(9), p 2929-2937
31. A.H. Wang, Z.Y. Tao, B.D. Zhu, J.M. Fu, X.Y. Ma, S.J. Deng, and X.D. Cheng, Laser Modification of Plasma-Sprayed Al_2O_3-13wt%TiO_2 Coatings on a Low-Carbon Steel, *Surf. Coat. Technol.*, 1992, **52**(2), p 141-144
32. K.M. Jasim, R.D. Rawlings, and D.R.F. West, Characterization of Plasma-Sprayed Layers of Fully Yttria-Stabilized Zirconia Modified by Laser Sealing, *Surf. Coat. Technol.*, 1992, **53**(1), p 75-86
33. A. Petitbon, L. Boquet, and D. Delsart, Laser Surface Sealing and Strengthening of Zirconia Coatings, *Surf. Coat. Technol.*, 1991, **49**(1-3), p 57-61
34. M. Inada, T. Maeda, and M. Inada, HIP of Plasma Spray Coated Ceramics, *Proceedings of International Symposium on Advanced Thermal Spraying Technology and Allied Coatings*, Japan High Temperature Society, 1988, p 211-215
35. K.A. Khor, Hot Isostatic Pressing Modifications of Pore Size Distribution in Plasma Sprayed Coatings, *Mater. Manuf. Processes*, 1997, **12**(2), p 291-307
36. C. Zhang, G. Zhang, S. Leparoux, H. Liao, C.-X. Li, C.-J. Li, and C. Coddet, Microwave Sintering of Plasma-Sprayed Yttria Stabilized Zirconia Electrolyte Coating, *J. Eur. Ceram. Soc.*, 2008, **28**(13), p 2529-2538
37. B.Z. Janos, E. Lugscheider, and P. Remer, Effect of Thermal Aging on the Erosion Resistance of Air Plasma Sprayed Zirconia Thermal Barrier Coating, *Surf. Coat. Technol.*, 1999, **113**(3), p 278-285
38. B. Prawara, H. Yara, Y. Miyagi, and T. Fukushima, Spark Plasma Sintering as a Post-Spray Treatment for Thermally-Sprayed Coatings, *Surf. Coat. Technol.*, 2003, **162**(2-3), p 234-241
39. J.A. Thompson and T.W. Clyne, The Effect of Heat Treatment on the Stiffness of Zirconia Top Coats in Plasma-Sprayed TBCs, *Acta Mater.*, 2001, **49**(9), p 1565-1575
40. A. Cipitria, I.O. Golosnoy, and T.W. Clyne, A Sintering Model for Plasma-sprayed Zirconia TBCs. Part I: Free-standing Coatings, *Acta Mater.*, 2009, **57**(4), p 980-992
41. A. Cipitria, I.O. Golosnoy, and T.W. Clyne, A Sintering Model for Plasma-sprayed Zirconia Thermal Barrier Coatings. Part II: Coatings Bonded to a Rigid Substrate, *Acta Mater.*, 2009, **57**(4), p 993-1003
42. N.N.K. Miyajima, Y. Harada, and H. Nakahira, Refining of Sprayed Oxide Coating by Chemically Densifying Method, *J. Jpn. High Temp. Soc.*, 1992, **18**(Suppl), p 307-313
43. C.-J. Li, C.-X. Li, and X.-J. Ning, Performance of YSZ Electrolyte Layer Deposited by Atmospheric Plasma Spraying for Cermet-Supported Tubular SOFC, *Vacuum*, 2004, **73**(3-4), p 699-703
44. C.-J. Li, X.-J. Ning, and C.-X. Li, Effect of Densification Processes on the Properties of Plasma-Sprayed YSZ Electrolyte Coatings for Solid Oxide Fuel Cells, *Surf. Coat. Technol.*, 2005, **190**(1), p 60-64
45. X.-J. Ning, C.-X. Li, C.-J. Li, and G.-J. Yang, Modification of Microstructure and Electrical Conductivity of Plasma-Sprayed YSZ Deposit Through Post-Densification Process, *Mater. Sci. Eng., A*, 2006, **428**(1-2), p 98-105
46. M. Vippola, S. Ahmaniemi, J. Keranen, P. Vuoristo, T. Lepisto, T. Mantyla, and E. Olsson, Aluminum Phosphate Sealed Alumina Coating: Characterization of Microstructure, *Mater. Sci. Eng., A*, 2002, **323**(1-2), p 1-8
47. K. Niemi, P. Sorsa, P. Vuoristo, and T. Mantyla, Thermal Spray Alumina Coatings with Strongly Improved Wear and Corrosion Resistance, *Thermal Spray Industrial Applications*, C.C. Berndt and S. Sampath, Ed., ASM International, 1994, p 533-536
48. E.M. Leivo, M.S. Vippola, P.P.A. Sorsa, P.M.J. Vuoristo, and T.A. Mantyla, Wear and Corrosion Properties of Plasma Sprayed Al_2O_3 and Cr_2O_3 Coatings Sealed by Aluminum Phosphates, *J. Therm. Spray Technol.*, 1997, **6**(2), p 205-210
49. S. Ahmaniemi, M. Vippola, P. Vuoristo, T. Mantyla, M. Buchmann, and R. Gadow, Residual Stresses in Aluminium Phosphate Sealed Plasma Sprayed Oxide Coatings and Their Effect on Abrasive wear, *Wear*, 2002, **252**(7-8), p 614-623
50. M. Vippola, S. Ahmaniemi, P. Vuoristo, T. Lepisto, T. Mantyla, and E. Olsson, Microstructural Study of Aluminum Phosphate-Sealed, Plasma-Sprayed Chromium Oxide Coating, *J. Therm. Spray Technol.*, 2002, **11**(2), p 253-260
51. M. Vippola, P. Vuoristo, T. Lepisto, and T. Mantyla, AEM Study of Aluminum Phosphate Sealed Plasma Sprayed Al_2O_3 and Cr_2O_3 Coatings, *J. Mater. Sci. Lett.*, 2003, **22**(6), p 463-466
52. T. Troczynski, Q. Yang, and G. John, Post-deposition Treatment of Zirconia Thermal Barrier Coatings Using Sol-Gel Alumina, *J. Therm. Spray Technol.*, 1999, **8**(2), p 229-234
53. B.R. Marple, J. Voyer, and P. Bechard, Sol Infiltration and Heat Treatment of Alumina-Chromia Plasma-sprayed Coatings, *J. Eur. Ceram. Soc.*, 2001, **21**(7), p 861-868
54. T. Mantyla, P. Vuoristo, and P. Kettunen, Chemical Vapor-Deposition Densification of Plasma-Sprayed Oxide Coatings, *Thin Solid Films*, 1984, **118**(4), p 437-444
55. V.A.C. Haanappel, J.B.A. Scharenborg, H.D. Vancorbach, T. Fransen, and P.J. Gellings, Can Thermal Barrier Coatings Be Sealed by Metal-Organic Chemical-Vapor-Deposition of Silica and Alumina, *High Temp. Mater. Processes (London)*, 1995, **14**(2), p 57-66
56. E. Lugscheider, P. Jokiel, V. Messerschmidt, and G. Beckschulte, Subsequent Sealing of Thermal Spray Coatings to Increase Corrosion Resistance, *Surf. Eng.*, 1994, **10**(1), p 46-51

57. B. Wielage, U. Hofmann, S. Steinhauser, and G. Zimmermann, Improving Wear and Corrosion Resistance of Thermal Sprayed Coatings, *Surf. Eng.*, 1998, **14**(2), p 136-138
58. H.J. Kim, C.H. Lee, and Y.G. Kweon, The Effects of Sealing on the Mechanical Properties of the Plasma-Sprayed Alumina-Titania Coating, *Surf. Coat. Technol.*, 2001, **139**(1), p 75-80
59. H.J. Kim, S. Odoul, C.H. Lee, and Y.G. Kweon, The Electrical Insulation Behavior and Sealing Effects of Plasma-Sprayed Alumina-Titania Coatings, *Surf. Coat. Technol.*, 2001, **140**(3), p 293-301
60. S. Liscano, L. Gil, and M.H. Staia, Correlation Between Microstructural Characteristics and the Abrasion Wear Resistance of Sealed Thermal-Sprayed Coatings, *Surf. Coat. Technol.*, 2005, **200**(5-6), p 1310-1314
61. S. Liscano, L. Gil, and M.H. Staia, Effect of Sealing Treatment on the Corrosion Resistance of Thermal-Sprayed Ceramic Coatings, *Surf. Coat. Technol.*, 2004, **188-189**, p 135-139
62. P. Ctibor, K. Neufuss, F. Zahalka, and B. Kolman, Plasma Sprayed Ceramic Coatings without and with Epoxy Resin Sealing Treatment and Their Wear Resistance, *Wear*, 2007, **262**(9-10), p 1274-1280
63. C.-J. Li, G.-J. Yang, and A. Ohmori, Potential Strengthening of Erosion Performance of Plasma-Sprayed Al_2O_3 Coating by Adhesives Impregnation, *J. Mater. Sci. Lett.*, 2003, **22**(21), p 1499-1501
64. H. Ito, R. Nakamura, and M. Shiroyama, Infiltration of Copper into Titanium-Molybdenum Spray Coatings, *Surf. Eng.*, 1988, **4**(1), p 35-38
65. A. Ohmori, Z. Zhou, and K. Inoue, Liquid-Mn Sintering of Plasma-Sprayed Zirconia Yttria Coatings, *Thin Solid Films*, 1994, **251**(2), p 141-146
66. A. Ohmori, Z. Zhou, K. Inoue, K. Murakami, and T. Sasaki, Penetration Treatment of Plasma-Sprayed ZrO_2 Coating by Liquid Mn Alloys, *J. Therm. Spray Technol.*, 1996, **5**(2), p 134-138
67. A. Ohmori, C.-J. Li, and Y. Arata, Fundamental Properties of the ACT-JP (Arata Coating Test with Jet Particles), *Thermal Spray: Advances in Coatings Technology*, D.L. Houck, Ed., 1987 (Orlando, FL), ASM International, 1988, p 79-83
68. J.F. Li and C.-X. Ding, Polishing-Induced Pull outs of Plasma Sprayed Cr_3C_2-NiCr Coating, *J. Mater. Sci. Lett.*, 1999, **18**(21), p 1719-1721
69. J. Karthikeyan, A.K. Sinha, and A.R. Biswas, Impregnation of Thermally Sprayed Coatings for Microstructure Studies, *J. Therm. Spray Technol.*, 1996, **5**(1), p 74-78
70. C.-J. Li, A. Ohmori, and R. McPherson, The Relationship Between Microstructure and Young's Modulus of Thermally Sprayed Ceramic Coatings, *J. Mater. Sci.*, 1997, **32**(4), p 997-1004
71. S. Kuroda and T.W. Clyne, The Quenching Stress in Thermally Sprayed Coatings, *Thin Solid Films*, 1991, **200**(1), p 49-66
72. Y. Arata, A. Ohmori, and C.-J. Li, Electrochemical Method to Evaluate the Connected Porosity in Ceramic Coatings, *Thin Solid Films*, 1988, **156**(2), p 315-325
73. C. Zhang, W.-Y. Li, M.P. Planche, C.-X. Li, H.L. Liao, C.-J. Li, and C. Coddet, Study on Gas Permeation Behaviour Through Atmospheric Plasma-Sprayed Yttria Stabilized Zirconia Coating, *Surf. Coat. Technol.*, 2008, **202**(20), p 5055-5061
74. A. Mirahmadi and K. Valefi, Densification of Plasma Sprayed SOFC Electrolyte Layer Through Infiltration with Aqueous Nitrate Solution, *J. Fuel Cell Sci. Technol.*, 2012, **9**(1), p 011001
75. R.J. Damani and P. Makroczy, Heat Treatment Induced Phase and Microstructural Development in Bulk Plasma Sprayed Alumina, *J. Eur. Ceram. Soc.*, 2000, **20**(7), p 867-888
76. C.-J. Li and W.-Z. Wang, Quantitative Characterization of Lamellar Microstructure of Plasma-Sprayed Ceramic Coatings Through Visualization of Void Distribution, *Mater. Sci. Eng., A*, 2004, **386**(1-2), p 10-19
77. J. Pech and B. Hannoyer, Influence of Oxide Layer Promoted by d.c. Plasma Preheating on the Adhesion Coating and Role of the Initial Surface Pretreatment, *Surf. Interface Anal.*, 2000, **30**(1), p 585-588
78. T. Chraska and A.H. King, Effect of Different Substrate Conditions upon Interface with Plasma Sprayed Zirconia—A TEM Study, *Surf. Coat. Technol.*, 2002, **157**(2-3), p 238-246
79. C.-J. Li and J.-L. Li, Evaporated-Gas-Induced Splashing Model for Splat Formation During Plasma Spraying, *Surf. Coat. Technol.*, 2004, **184**(1), p 13-23
80. X.Y. Jiang, Y.P. Wan, H. Herman, and S. Sampath, Role of Condensates and Adsorbates on Substrate Surface on Fragmentation of Impinging Molten Droplets During Thermal Spray, *Thin Solid Films*, 2001, **385**(1-2), p 132-141
81. W. Funk, F. Goebe, and M. Mauz, The Influence of Substrate Temperature on the Bonding Strength of Plasma Sprayed Oxide Ceramics, *Proceedings of 1st Plasma-Technik-Symposium, Plasma-Technik AG*, Wohlen, Switzerland, 1988, p 59-66
82. G. Barbezat, and K. Landes, Plasma Technology Triplex for the Deposition of Ceramic Coatings in the Industry, *Thermal Spray: Surface Engineering Via Applied Research*, C.C. Berndt, Ed., 2000 (Montreal, Quebec, Canada), ASM International, 2000, p 881-885
83. G. Barbezat, The Internal Plasma Spraying on Powerful Technology for the Aerospace and Automotive Industries, Thermal Spray 2001: New Surfaces for a New Millennium, C.C. Berndt, K.A. Khor, and E.F. Lugscheider, Ed., 2001 (Singapore), ASM International, 2001, p 135-139
84. C.R.C. Lima and J.M. Guilemany, Adhesion Improvements of Thermal Barrier Coatings with HVOF Thermally Sprayed Bond Coats, *Surf. Coat. Technol.*, 2007, **201**(8), p 4694-4701
85. W. Shen, F.C. Wang, Q.B. Fan, Z.A. Ma, and X.W. Yang, Finite Element Simulation of Tensile Bond Strength of Atmospheric Plasma Spraying Thermal Barrier Coatings, *Surf. Coat. Technol.*, 2011, **205**(8-9), p 2964-2969
86. S.A. Sadeghi-Fadaki, K. Zangeneh-Madar, and Z. Valefi, The Adhesion Strength and Indentation Toughness of Plasma-sprayed Yttria Stabilized Zirconia Coatings, *Surf. Coat. Technol.*, 2010, **204**(14), p 2136-2141
87. C.-J. Li and A. Ohmori, Influence of Plasma Spray Conditions on the Structure of Al_2O_3 Coatings, *Trans. Jpn. Weld. Res. Inst.*, 1990, **19**, p 259-270
88. C.-J. Li, G.-J. Yang, and A. Ohmori, Relationship Between Particle Erosion and Lamellar Microstructure for Plasma-Sprayed Alumina Coatings, *Wear*, 2006, **260**(11-12), p 1166-1172
89. Y.I. Oka, S. Mihara, and T. Yoshida, Impact-Angle Dependence and Estimation of Erosion Damage to Ceramic Materials Caused by Solid Particle Impact, *Wear*, 2009, **267**(1-4), p 129-135
90. H.M. Hawthorne, L.C. Erickson, D. Ross, H. Tai, and T. Troczynski, The Microstructural Dependence of Wear and Indentation Behaviour of some Plasma-Sprayed Alumina Coatings, *Wear*, 1997, **203**, p 709-714
91. A. Ohmori, and C.-J. Li, Evaluation of the Lamellar Bonding of Ceramic Coating by Particle Erosive Test, *Thermal Spraying: Current Status and Future Trends*, A. Ohmori, Ed., 1995 (Kobe, Japan), High Temperature Society of Japan, 1995, p 967-972